Published in final edited form as:
Curr Biol. 2009 February 24; 19(4): 277–286. doi:10.1016/j.cub.2009.01.039.

An alveolate specific dynamin is required for the biogenesis of specialised secretory organelles in *Toxoplasma gondii*

Manuela S. Breinich[1], **David J.P. Ferguson**[2], **Bernardo J. Foth**[3], **Giel G. van Dooren**[4], **Maryse Lebrun**[5], **Doris V. Quon**[6], **Boris Striepen**[4], **Peter J. Bradley**[6], **Friedrich Frischknecht**[1], **Vernon B. Carruthers**[7], and **Markus Meissner**[1,*]

[1]Hygiene Institute, Department of Parasitology, Heidelberg University School of Medicine, Heidelberg, Germany

[2]Nuffield Department of Pathology, University of Oxford, John Radcliffe Hospital, Oxford OX3 9DU, United Kingdom

[3]School of Biological Sciences, Nanyang Technological University, 60 Nanyang Drive, Singapore 637551

[4]Center for Tropical and Emerging Global Diseases and Department of Cellular Biology, University of Georgia, Athens, 30602, GA, USA

[5]INSERM, UMR 55235 CNRS, Université de Montpellier 2, CP 107, Place Eugène Bataillon, 34090 Montpellier, France

[6]Department of Microbiology, Immunology and Molecular Genetics, University of California, Los Angeles, Los Angeles CA 90095-1489 USA

[7]Department of Microbiology and Immunology, University of Michigan School of Medicine, Ann Arbor, Michigan 48109, USA

Summary

Background—Apicomplexans contain only a core set of factors involved in vesicular traffic. Yet these obligate intracellular parasites evolved a set of unique secretory organelles (micronemes, rhoptries and dense granules) that are required for invasion and modulation of the host cell. Apicomplexa replicate by budding from or within a single mother cell and secretory organelles are synthesised *de novo* at the final stage of division. To date the molecular basis for their biogenesis is unknown.

Results—We demonstrate that the apicomplexan dynamin related protein B (DrpB) belongs to an alveolate specific family of dynamins that is expanded in ciliates. DrpB accumulates in a cytoplasmic region close to the Golgi that breaks up during replication and reforms after assembly of the daughter cells. Conditional ablation of DrpB function results in mature daughter parasites that are devoid of micronemes and rhoptries. In the absence of these organelles invasion related secretory proteins are mistargeted to the constitutive secretory pathway. Mutant parasites are able to replicate but are unable to escape from or invade into host cells.

Conclusion—DrpB is the essential mechanoenzyme for the biogenesis of secretory organelles in Apicomplexa. We suggest that DrpB is required during replication to generate vesicles for the regulated secretory pathway that form the unique secretory organelles. Our study supports a role of an alveolate specific dynamin that was required for the evolution of novel, secretory organelles. In the case of Apicomplexa these organelles further evolved to enable a parasitic lifestyle.

*Correspondence should be sent to: Markus Meissner, (markus.meissner@med.uni-heidelberg.de).

Introduction

To adapt to a parasitic lifestyle Apicomplexa evolved a whole set of unique secretory organelles (micronemes, rhoptries and dense granules) that contain crucial factors for invasion and modulation of the host cell [1].

Proteins destined to these organelles are sorted in the secretory pathway and sequence motifs for the targeting to the rhoptries and micronemes have been identified [2]. Rhoptry and microneme proteins are transported via endosomal like compartments where proteolytic maturation takes place [3, 4]. Correct trafficking of secretory proteins depends on appropriate timing of expression [4, 5], which indicates that their transport is linked to organellar biogenesis.

The mechanisms involved in biogenesis and maintenance of these organelles are unknown. Given the complex cellular organisation of Apicomplexa, one would predict that an expansion of trafficking proteins occurred, similar to other complex eukaryotes [6]. However, apicomplexan parasites contain only a core set of trafficking factors, for example Rab-GTPases [7], SNAREs and vesicle coats[8].

Apicomplexa replicate within a single mother cell and secretory organelles are synthesised *de novo* at the final stage of division [9]. They are at least partially derived from the Golgi [10, 11] and coated vesicles have been observed at Golgi stacks that might be transported to micronemes or rhoptries [12].

Dynamins are large GTPases that are involved in numerous cellular processes [13]. While classical dynamins are required for scission of vesicles by acting as mechanoenzymes or molecular switches [14, 15], dynamin related proteins (Drp) have diverse functions, including division of organelles or vesicular traffic [13]. We identified three Drp genes in the genome of apicomplexan parasites, termed here DrpA, DrpB and DrpC. Interestingly DrpB belongs to a class that is conserved within the alveolates and shows a lineage specific expansion in ciliates [16]. Similar to apicomplexans, ciliates contain specialised secretory organelles (i.e. trichocysts, exocyts, extrusomes; see [17]) and a common ancestry has been suggested based on ultrastructural similarities [18].

We demonstrate here the functional role of DrpB in *Toxoplasma gondii*. We found that DrpB accumulates in a novel cytoplasmic assembly close to the Golgi and that this accumulation disperses during replication. We found that conditional ablation of DrpB function results in parasites deprived of specialised secretory organelles and demonstrate that these mutants replicate normally inside the host but are incapable of host cell egress, gliding motility and invasion. DrpB appears to function in a discrete step during replication of the parasite that leads to the formation of secretory organelles. Given that DrpB is the only member of this otherwise expanded dynamin family in apicomplexan parasites we speculate that the original role in alveolates lies in the biogenesis of specialised secretory organelles. In the case of Apicomplexa these organelles further evolved to enable a parasitic lifestyle.

Results

Apicomplexa contain three dynamin related proteins

We identified three highly conserved, dynamin related proteins (DrpA, B, C) in the apicomplexan genome databases (www.apiDB.org). DrpA and DrpB show a typical domain organisation, consisting of a conserved N-terminal GTPase domain, a middle domain and a GTPase effector domain (GED). In contrast DrpC contains only a recognisable GTPase

domain, similar to dynamins known to be involved in chloroplast division, such as ARC5 of *Arabidopsis thaliana* [19] (Fig. 1A). We performed a phylogenetic analysis using an alignment of conserved regions and including dynamins from diverse organisms (accession numbers and alignments can be downloaded as supplementary data). DrpA, B and C fall into three distinct clades with high bootstrap support. While homologues for DrpA and B were identified in other alveolates (Fig. 1B), DrpC formed an apicomplexan specific clade (supplementary Figure 1)

DrpB resides near the Golgi and endosomal associated compartments

Antibodies raised against DrpB specifically recognised a protein of the expected size (95 kDa) in wild type (RH) parasite lysates (supplementary Figure 2 and Fig. 1D,E). We were not able to co-localise DrpB with markers of the secretory pathway, such as the cis/medial Golgi marker GRASP-RFP [20], the trans-Golgi marker UDP-*N*-acetyl-D-galactosamine: polypeptide *N*-acetylgalactosaminyltransferase T1 fused to yellow fluorescent protein (YFP) (TgGalNac-YFP; Nishi and Roos, unpublished data) [4], the pro-peptide of M2AP (a precursor microneme protein that localises in endosomal related compartments)[4], VP-1 (a vacuolar proton pyrophosphatase) [4] or the μ1 chain of the adaptin-1 complex [3] (Fig. 1C).

To corroborate the observed location with biochemical fractionations, we lysed extracellular parasites in PBS and separated proteins into soluble and insoluble fractions. Under these conditions we found that DrpB is almost completely insoluble and can only be partially solubilised by detergent extraction (2% Triton X-100) (Fig. 1D). Together these data indicated that a significant amount of insoluble DrpB is accumulated close to the Golgi and endosomal-like compartments. Since we failed to reveal the location of DrpB in immuno-electron analysis with DrpB-antibody, we decided to gain more insight into the location and function of DrpB by analysing transgenic parasites that express different GFP-tagged versions of DrpB (supplementary Figure 1).

While we were able to generate parasites constitutively expressing GFP-DrpB (supplementary Figure 2), our attempts to generate parasites expressing a truncated version of DrpB ($DrpB_{DN}$), where the GTPase domain is deleted failed. This confirmed previous reports, suggesting that the deletion of the GTPase domain results in a dominant negative dynamin[21]. We applied the ddFKBP-system that allows a tunable regulation of protein levels [22]. Fusion of ddFKBP-GFP to full length DrpB (dd-$DrpB_{wt}$) and $DrpB_{DN}$ (dd-$DrpB_{DN}$) allowed generation of transgenic parasite strains. Efficient Shield-1(Shld-1) dependent regulation of the respective protein levels (dd-$DrpB_{wt}$ and dd-$DrpB_{DN}$) was confirmed in immunoblot and immunofluorescence analysis (Fig. 1E,F). We detected dd-$DrpB_{WT}$ as soon as 3 hours after addition of 0.01 μM Shld-1 (Fig. 1F). Irrespective of the expression levels of dd-$DrpB_{wt}$ or dd-$DrpB_{DN}$ we detected the protein at the same location as endogenous DrpB, close but distinct to the Golgi (Fig. 1F and supplementary Figure 2). Strong overexpression and longer induction times resulted in an enlarged, spherical appearance of the respective signal and a significant accumulation of the respective constructs in the residual body (supplementary Figure 3), a remnant of the mother after parasite division.

Immuno-electron microscopy on parasites expressing GFP-DrpB (Fig. 2) or dd-$DrpB_{DN}$ (supplementary Figure 3) revealed an accumulation of GFP-DrpB close to the Golgi that appeared spherical and did not seem to have a membrane (Fig. 2A, insert). At the start of daughter formation we observed more dispersed gold particles and loss of the material indicating that it breaks up during replication (Figs.2B, C). Indeed, most cells undergoing division did not exhibit this accumulation (not shown). Towards the end of replication we detected the reformation of the homogenous material within each daughter (Figs.2D, E, F).

We conclude that DrpB is concentrated in an insoluble cytosolic pool close to the Golgi that disassembles during the replication of the parasite (see also supplementary movie).

Parasites expressing dominant negative DrpB are paralysed

We analysed parasites conditionally expressing dd-DrpB$_{DN}$. Stabilisation of dd-DrpB$_{DN}$ resulted in parasites that were unable to form plaques in a monolayer of human foreskin fibroblasts (HFF), indicating an essential function of DrpB. In contrast, expression of dd-DrpB$_{wt}$ or GFP-DrpB had no significant effect on parasite growth (Fig. 3A).

We found no significant difference in replication, as indicated by a similar number of parasites per parasitophorous vacuole (PV) (Fig. 3B). When parasites were treated with Shld-1 for 36 hours, mechanically released from the host cell and analysed for their ability to invade host cells, we found that invasion in parasites expressing dd-DrpB$_{DN}$ was blocked (85%), when compared to control parasites (Fig. 3B). In contrast, we did not find any differences in invasion when extracellular parasites were treated with Shld-1 for 6 hours, although strong expression of dd-DrpB$_{DN}$ was detectable (data not shown).

Next we analysed parasite egress from the host cell. Parasites were grown for 36 hours in presence or absence of Shld-1 and subsequently egress was triggered using the calcium-ionophore A23187 [23]. Even a prolonged incubation with A23187 for up to 15 minutes was not sufficient to trigger egress if dd-DrpB$_{DN}$ was stabilised (Fig. 3C).

Next we analysed the parasite's ability to move by gliding motility, which is essential for invasion of the host cell[24]. We employed a qualitative trail deposition assay [25] and found that Shld-1 treatment for 36 hours during replication resulted in paralysed dd-DrpB$_{DN}$-parasites. Occasionally short trails were detected in this assay (Fig. 3D). In contrast ~20% of non-induced parasites formed trails. Stabilisation of dd-DrpB$_{DN}$ in extracellular parasites had no effect on gliding motility (data not shown).

Together our phenotypic characterisation demonstrates that functional DrpB is required for host cell egress, gliding motility and host cell invasion. While DrpB appears to be required during the intracellular development of the parasite, it is not necessary for parasite replication.

DrpB functions in the secretory pathway

Drps are involved in mitochondria and plastid segregation in various organisms [19]. However, we found that expression of DrpB$_{DN}$ had no effect on replication and segregation of mitochondrion, plastid or Golgi (Fig. 1F and supplementary Figure 4).

We analysed if expression of DrpB$_{DN}$ affects the secretory pathway. We did not observe effects on the location of the major surface antigen SAG1, indicating that the constitutive secretory pathway is not affected (Fig. 4A).

A specific effect on the location of proteins transported to the specialised secretory organelles (micronemes, rhoptries and dense granules) was evident. We found that micronemal and rhoptry proteins are re-routed to the constitutive secretion (default) pathway. No staining of the respective organelles was achieved using several known markers. Instead we identified these proteins either in the lumen of the parasitophorous vacuole or at the plasma membrane (Fig. 4A). A significant effect was also seen for proteins residing in dense granules, since fewer intracellular dense granules were detected upon expression of dd-DrpB$_{DN}$ (Fig. 4A). We noted a different fate of micronemal transmembrane proteins once they reach the surface of the parasite. Whereas MIC2 and 6

were secreted into the lumen of the PV, MIC8 remained at the surface of the parasite (Fig. 4B).

To confirm that expression of dd-DrpB$_{DN}$ causes a specific effect on the secretory pathway, we analysed parasites expressing an independent dynamin mutant. Expression of dynamins with mutations in the GTP-binding site have been shown to specifically disrupt dynamin function [13]. We generated a dominant-negative DrpB where a lysine in the GTP-binding site was changed to an alanine (K72A). As expected, expression of dd-DrpB$_{K72A}$ in *T. gondii* resulted in the same re-routing of secretory proteins as observed for dd-DrpB$_{DN}$ (supplementary Figure 3 and data not shown).

Proteolytic maturation of secretory proteins is partially impaired

It has been demonstrated that proteolytic maturation of micronemal and rhoptry proteins occurs during their transport in endosomal-like compartments as shown for M2AP [4] and RON8 (Lebrun et al., not published). Pro-peptides can be detected in these compartments using antibodies raised against proM2AP or proRon8. We were interested if micronemal and rhoptry proteins are still routed via these compartments. We found that expression of dd-DrpB$_{DN}$ results in a complete loss of the typical proM2AP and pro-RON8 signal. Instead we obtained significant labelling of the PV lumen, indicating that they are constitutively secreted (Fig. 4C). In immunoblot analysis we detected fewer amounts of the mature forms of M2AP (40 kDa) and MIC6 (45 kDa) respectively, indicating that proteolytic processing is affected in Shld-1 treated dd-DrpB$_{DN}$-parasites. However, proteolytic maturation still occurred (Fig. 4D). It is possible that under conditions of dd-DrpB$_{DN}$ expression no transport via the endosomal compartments occurs and that the protease(s) required for proteolytic maturation of micronemal and rhoptry proteins are transported via the same route as their substrate.

DrpB is essential for organelle biogenesis

We analysed parasites 12 hours after addition of Shld-1 and observed a mixed population of parasites. While some parasites still showed normal location of micronemal or rhoptry proteins, others showed the typical mislocalisation (Fig. 5 and data not shown). Interestingly, single parasites showed a normal location, indicating that at least one round of replication is required for the re-routing of secretory proteins. Biogenesis of secretory organelles occurs during a late stage of daughter cell development, coinciding with the disappearance of the respective organelles in the mother cell [9]. To study the function of DrpB during replication we introduced MIC8-tagged to mCherry into dd-DrpB$_{DN}$-parasites and followed the fate of micronemes during replication. We inoculated parasites in presence of Shld-1 for 8 hours to stabilise dd-DrpB$_{DN}$ before time lapse analysis. Although single parasites showed strong expression levels of dd-DrpB$_{DN}$, we found that MIC8 was still localised normally in the micronemes, indicating that rerouting of the micronemal proteins to the constitutive secretion pathway had not taken place at this time (Fig. 5A,B and supplementary movie). During replication we found that micronemes in the mother cell disappear as observed previously ([9] and Fig. 5A). In contrast to non-induced parasites no formation of novel micronemes was evident in the forming daughter parasites (Fig. 5A). At a later time point MIC8-mCherry was detected at the surface of the fully assembled daughter parasites (Fig. 5A,B and supplementary movie).

During the replication we observed an impressive change in the organisation of DrpB localisation (Fig. 5A). A portion of the DrpB-GFP appeared to break off from its pool into smaller structures as they relocated towards the posterior pole of the parasite. After completion of replication DrpB was found again in discrete spots in both daughters and in the residual body (Fig. 5A). These data confirmed the observations on DrpB localisation by

IEM (Fig. 2). Based on these results we conclude that DrpB is required for *de novo* biogenesis of secretory organelles during the replication of the parasite.

Ultrastructural analysis of parasites expressing $DrpB_{DN}$

We performed ultrastructural studies on parasites expressing dd-$DrpB_{DN}$, treated for 12, 24 and 36 hours in presence or absence of Shld-1 prior to fixation. In untreated samples, increasing numbers of tachyzoites with time were observed within the parasitophorous vacuoles. These parasites were slightly teardrop-shaped with a normal compliment of organelles including groups of rhoptries, a number of micronemes and dense granules (Fig. 6A). In contrast, in the treated samples, the tachyzoites appeared elongated and thinner and were in loose vacuoles containing large amounts of the tubular structures compared to the untreated control (Fig. 6A and B). In the treated sample it was possible to observe parasites at various stages of endodyogeny and repeated endodyogeny, which appeared normal (not shown). However, in the fully formed tachyzoites it was difficult to identify apical organelles (Fig. 6C). The conoid was present and a few duct-like structures were visible (Fig. 6C) but only rarely was the bulb-like portion of a rhoptry observed. Similarly it was difficult to identify microneme-like structures but there were few dense granules within the cytoplasm (Fig. 6C). Detailed examination of the anterior end of the tachyzoite, showed a normal appearing mitochondrion, apicoplast and Golgi body giving rise to numerous vesicles (Fig. 6D, E). In addition certain parasites, anterior to the Golgi body, were electron lucent vacuolar structures (Fig. 6E) or clumps of electron dense homogenous material (Fig. 6D).

Discussion

To adapt to a parasitic lifestyle, apicomplexans evolved unique specialised organelles that contain numerous proteins required for invasion, modulation and lysis of the host cell. Consequently the specific transport of virulence factors localised in these organelles has been of considerable interest [2]. Although much of the previous work focused on trafficking signals that facilitate the transport of the respective proteins to micronemes or rhoptries, the mechanisms involved in their biogenesis and maintenance have been unknown. Protein sorting to the rhoptries involves an evolutionary conserved tyrosine dependent sorting motif that has been reported to interact with the adaptor molecule AP-1 [3, 26]. Similarly in case of micronemal proteins sequence motifs in the cytosolic tail domains of transmembrane proteins are necessary for targeting a protein to the micronemes [27].

Another common feature of protein transport to micronemes and rhoptries is the importance of pro-peptides and their processing that is involved in protein sorting, as shown for micronemal proteins such as M2AP, MIC3 and MIC5 [4, 5, 28] and rhoptry proteins like ROP1 [29] [30]. Interestingly, it has been documented that timing of expression plays a crucial role for organellar targeting. For example, a recent study on the trafficking of MIC3 demonstrated cell cycle dependent transport [5]. These similarities in protein sorting indicate common, tightly regulated mechanisms for the transport of proteins to the specialised secretory organelles.

In this study we show that the biogenesis of micronemes, rhoptries (and possibly dense granules) requires functional DrpB during parasite replication. In absence of functional DrpB parasites are able to replicate but do not form secretory organelles *de novo.* Previously it has been shown that depletion of functional AP-1 using anti-sense technology affects biogenesis of rhoptries which leads to distorted parasites, unable to replicate [3]. In sharp contrast, we demonstrate here that parasites devoid of secretory organelles replicate normal inside the host cell. This contradiction can be explained by additional functions of AP-1

during intracellular replication, unrelated to rhoptry biogenesis. Alternatively the anti-sense technology as employed to deplete functional AP-1 might be not prone to off-target effects.

We show here that parasites devoid of specialised secretory organelles are completely paralysed regarding host cell egress, gliding motility and invasion. Interestingly the function of DrpB appears to be not required in extracellular, non dividing parasites, since stabilisation of trans-dominant DrpB in this stage does not result in reduced invasion or gliding motility. In contrast, when we followed the fate of micronemal proteins and rhoptries in dividing, intracellular parasites, we found that they are not targeted to their respective organelle. Instead these proteins enter the constitutive secretion pathway (default pathway). Using several molecular markers we confirmed that the observed effect is specific for the secretory organelles, since no differences in the protein transport to the IMC, Golgi or plasma membrane has been detected. In ultrastructural analysis we confirmed a specific effect on the secretory organelles (micronemes, rhoptries and dense granules).

In non-replicating (extracellular) parasites DrpB is almost completely insoluble and shows a distinct localisation close but distinct to the Golgi. In fact it seems that DrpB localises in a previously unnoticed cytosoplasmic accumulation close to the Golgi. We confirmed that this accumulation breaks up during replication of the parasite in IEM and time-lapse analysis. In fact a very dynamic process was evident during the course of replication and a reassembly of the accumulation occurring after the formation of mature daughter parasites. We speculate that DrpB concentrates in an inactive pool in resting parasites that becomes rapidly activated during replication. After biogenesis of the organelles DrpB reassociates in an inactive pool. Although further experiments are required to identify interacting partners that are involved in the regulation of DrpB activity, we speculate that it's activation is regulated by cell cycle dependent factors, similar to the regulation of Drps required for mitochondrial division [31]. Accordingly we identified conserved phosphorylation sites for the cyclin dependent kinases in apicomplexan DrpBs (data not shown). The disassembly of the DrpB-pool coincides with the period when micronemes of the mother disappear and novel micronemes are formed within the daughter cells. A similar correlation was evident in static immunofluorescent assays for the biogenesis of the rhoptries (data not shown).

In conclusion we show that DrpB is essential for the biogenesis of secretory organelles in *T. gondii*. We suggest that DrpB is required to form vesicles for the regulatory secretory pathway. Indeed previous studies showed that dynamins are involved in a number of functions including the formation of distinct vesicles [32]. We identified three dynamin related proteins in the genome of apicomplexan parasites and show that DrpB is closely related to an expanded family of ciliate specific dynamins. It has previously been demonstrated that Drp1 of *T. thermophila* functions in endocytosis. In this report the authors demonstrate that TtDrp1 represents an example of convergent evolution [16]. It thus appears that the lineage specific expansion of this dynamin class enabled ciliates to develop a higher complexity of membrane trafficking, similar to observations made in higher eukaryotes [6]. Based on our findings we speculate that the original function of this class of dynamins is the biogenesis of specialised secretory organelles in alveolates that have been a prerequisite to adapt a parasitic lifestyle.

Experimental Procedures

Parasite cell lines and selections

T. gondii tachyzoites (RH *hxgprt*$^{-}$) were grown in human foreskin fibroblasts (HFF) and maintained in Dulbecco's modified Eagle's medium (DMEM) supplemented with 10% fetal calf serum, 2 mM glutamine and 25 μg/ml gentamycine. To generate stable transformants, 5

× 10^7 freshly released RH*hxgprt*$^-$ parasites were transfected and selected as previously described [24]

Generation of Antibodies to Recombinant DrpB

For production of anti-DrpB antibodies, the region encoding residues 265–662 of DrpB was expressed in *Escherichia coli* as a hexahistidine fusion. Primers P1 (GGCCGAATTCCTGCGACTCGGATACACAGGA) and P2 (CCGGAAGCTTTTCTCTTGCAGCTGGCGCACCAG) were used for amplification of *T. gondii* Prugnaiud strain cDNA. The product was cloned using *Hind*III and *Eco*RI sites into the pET28a (Novagen) vector that encodes a C-terminal hexahistidine tag for rapid purification. The plasmid was sequenced and then transformed into *E. coli* BL21DE3 cells for expression. Bacteria containing the expression construct were grown to an A_{600} of 0.6 and induced with 1 mM isopropyl 1-thio-D-galactopyranoside for 5 h. Hexahistidine-tagged DrpB was purified using nickel-agarose (Qiagen) under denaturing conditions and eluted using low pH according to the manufacturer's instructions. Eluted proteins were dialyzed against PBS and 50ug was injected per immunization into a BALB/c mouse. Polyclonal antiserum was collected after the second boost and screened by IFA and Western blot analysis.

Generation of constructs

Full length cDNA encoding full length DrpB has been amplified using Oligo DrpB-s (5′-ACCGGTGGTATGGACGGCAAACGCGAGGA) and DrpB-as (5′-ATGCATTTAGTCGCTGAACAGCGGATT). Truncated cDNA encoding $DrpB_{DN}$ with DrpB-s2 (5′-ACCGGTGGTGAAATCAAACGCGAAATTTCCA) and DrpB-as2 (5′-atgcatTTAGTCGCTGAACAGCGGATT). The products were digested with NsiI and AgeI and ligated into the XmaI and PstI sites of pCTG [33]). This placed DrpB downstream of GFP expressed from a tub promoter. Subsequently the promoter regions were exchanged for tub-ddFKBP from vector tubDDmycYFP-CAT [22] placing DrpB under control of ddFKBP-system. Stable cell lines were generated using chloramphenicole selection. The expression construct encoding dd-$DrpB_{K72A}$ was generated by amplification and ligation of two cDNA-fragments using DrpB-s3 (5′-CCTTAATTAATCGCTGAACAGCGGATTG), K72A-as (5′-CCTTAATTAACCCCACGACGCAGATCCTAGGCAACTGGATAAACTGCTGAAGACC) and DrpB-as3 (5′-CCTTAATTAATCGCTGAACAGCGGATTG) and K72A-s (5′-CCCCTAGGATCTGCGTCGTGGGGACACAGTCCGCAGGCGCAAGCTCCGTTTTGG). The full length cDNA was subsequently introduced into vector p5RT70DDmycGFP-HX.

To generate cell lines co-expressing DrpB-constructs with apicoplast-targeted FNR-RFP [20], GRASP-RFP [20] or mitochondrial targeted HSP60-RFP (von Dooren et al., this issue), we co-transfected the respective construct with pDHFR and used pyrimethamine selection [34]. To generate cell lines co-expressing dd-$DrpB_{DN}$ and micronemal targeted MIC8-mCherry the ORF of mCherry[35] was amplified with Oligo Cherry-s (5′-GCCCTAGGGCAGCAGCAGCAGCAGCAATGGTGAGCAAGGGCGAGGAGG) and mCherry-as (5′ CGCCTAGGCTTGTACAGCTCGTCCATGCCGCCGGTG) and inserted into the single AvrII site of the construct pMIC8MIC8myc [36]. Co-transfection with pDHFR was employed to generate stable parasites [37]. To localise Tgμ1 [3], we introduced a Ty-tag between codons 231 and 232 by ligation of two cDNA fragments using mu1Ty-as (5′-CCCTGCAGATCGAGCGGGTCCTGGTTCGTGTGGACCTCCAACTTCGACACCGTGCGCCCTGAGGTCTCGAG), mu1-s (5′CCGAATTCCCTTTTTCGACAAAATGGCGGGGGCGTCTGCGGTGTTTATC) and mu1-s2 (5′-

CCGAATTCCCTTTTTCGACTGCAGGGGAAGGCCATCGAAATGGAGGACATC), mu1-as (5′-CCTTAATTAACTAGGAGAGTCTCAGTTGGTAC) respectively. Full length cDNA was subsequently introduced into the EcoRI/PacI site of vector p5RT70mycGFP-HX.

Immunofluorescence analysis

For immunofluorescence analysis of *T. gondii* HFF cells grown on cover slips were inoculated with parasites in presence or absence of Shld-1 for 12–36 hours. Cells were fixed either with 4% paraformaldehyde or −20°C methanol for 20minutes. Fixed cells were permeabilized with 0.2% Triton X-100 in PBS for 20 minutes and blocked in 2% bovine serum albumin in PBS for 20 minutes. Staining was performed using different sets of primary antibodies for 60 min and followed by Alexa-Fluor-594-conjugated goat anti-rabbit or Alexa-Fluor-488-conjugated goat anti-mouse antibodies for another 60 min, respectively (Molecular Probes). Z-stack images of 0.15 μm increment were collected on a PerkinElmer Ultra-View spinning disc confocal Nikon Ti inverted microscope, using a 100 × NA 1.6 oil immersion lens. Images were further processed using ImageJ 1.34r software. Time lapse analysis was performed as previously described [22]. Treated and untreated culture dishes were transferred to the stage of a Zeiss an inverted microscope (Axiovert 200M “Cell observer”) with a temperature and CO_2 controlled incubator at 37°C and 5% CO_2. Images were captured with an AxioCam HRm (Zeiss). Image acquisition was performed with Axiovision (Zeiss).

Cell Fractionation

Freshly egressed wild type parasites were colleted and washed once with PBS. Pellets of 10^8 parasites each were resuspended into 300 μl of buffer (PBS, PBS containing 1 M NaCl, PBS containing 0.1 M Na_2CO_3 (pH 11.5) and PBS containing 2% Triton X-100) lysed by freezing and thawing followed by sonication. Homogenates were separated into insoluble and soluble fractions by ultracentrifugation for 2 h at 100.000 g and 4°C. Samples of the supernatant and pellet fractions equivalent to 1×10^7 parasites were analysed by SDS-Page followed by immunoblot analysis.

Immunoblot analysis

Parasites were cultivated for 36 hours in the absence or presence of Shld-1. Subsequently parasites were harvested and washed twice in ice cold PBS. SDS-PAGE and Western Blot analysis of total parasite lysates were performed as described previously [38], using 6–12% polyacrylamide gels under reducing condition with 100 mM DTT. Per experiment an equal number of $0{,}5\times10^7$–1×10^7 parasites were loaded. For detection the indicated antibodies were used.

Growth assays

The plaque assay was performed as described before [24]. Monolayers of human foreskin fibroblasts (HFF), grown in 6 well plates, were infected with 50 tachyzoites per well. After one week of incubation at normal growth conditions (37°C, 5% CO2), cells were fixed 10 minutes with −20°C methanol 100%, stained with Giemsa stain for 10 minutes and washed once with PBS. Documentation was performed with a Nikon SMZ 1500.

Replication and Invasion

Assay was performed as previously described [24]. Briefly, 5×10^6 freshly released parasites, grown in presence or absence of Shld-1, were allowed to invade for 1 hour. Subsequently three washing steps to remove extracellular parasites were performed. Cells were then further incubated for 18 hours in presence and absence of Shld-1 before fixation. The number of vacuoles representing successful invasion events was determined in 20 fields of

view and the number of parasites per vacuole was determined. The number of vacuoles represents a percentage of 100% (which reflects successful invasion) in RH_{WT}. Mean values of three independent experiments +/− S.D. have been determined.

Egress assay

Parasites were grown for 36 hours on human foreskin fibroblasts in presence or absence of Shld-1. After short periods of treatment with A23187 (5 to 15 minutes), cells were fixed and stained with antibodies to SAG1, and analyzed by microscopy.

Gliding assay

Trail deposition assays have been performed as described before [25]. Briefly parasites were grown for 36 hours in presence or absence of Shld-1. Freshly released parasites were allowed to glide on FCS-coated glass slides for 30 minutes before they were fixed with 4% PFA and stained with SAG1.

Electron microscopy

Monolayers were infected with dd-$DrpB_{DN}$ parasites and culture for 12, 24 and 36 hours in the presence or absence of Shld-1 prior to fixation in 4% glutaraldehyde in 0.1M phosphate buffer and processed for routine electron microscopy as described previously [39]. In summary samples were post-fixed in osmium tetroxide, dehydrated, treated with propylene oxide and embedded in Spurr's epoxy resin. Thin sections were stained with uranyl acetate and lead citrated prior to examination in a JEOL 1200EX electron microscope.

For immuno-electron microscopy, a sample of cells infected with DrpB-GFP parasites was fixed in 2% paraformaldehyde. The sample was dehydrated and embedded in LR White acrylic resin. For immuno-staining thin section on nickel grids were floated on drops of 1% BSA in PBS to block non-specific staining. Grids were then floated on drops containing rabbit anti-GFP, washed and then exposed to anti-rabbit Ig conjugated to 10nm gold particles. After washing sections were stained with uranyl acetate prior to examination in the electron microscope.

Phylogenetic analysis

Dynamin protein sequences were retrieved from GenBank and the Joint Genome Institute (http://genome.jgi-psf.org). After randomizing sequence order an alignment was created with ClustalX v1.83 using the default Pairwise and Multiple Alignment Parameters. Alignment positions containing >20% gaps were excluded before carrying out phylogenetic analysis using the PHYLIP v3.65 programs PROML, PROTDIST and NEIGHBOR, SEQBOOT, and CONSENSE. PROTDIST and PROML were run employing the Jones–Taylor–Thornton amino acid substitution matrix, and gamma distribution parameters for six variable rate categories were estimated with TREEPUZZLE v5.2 [40]. Where available sequence input order was randomized before starting PHYLIP programs. For bootstrapping 100 re-sampled replicates were generated with SEQBOOT and an unrooted Majority Rule consensus tree was calculated with CONSENSE. Phylogenetic trees were visualized with TREEVIEW v1.6.6 [41].

Supplementary Material

Refer to Web version on PubMed Central for supplementary material.

Acknowledgments

We are grateful to C. Beckers, D. Soldati-Favre, M.-F. Cesbrauw, J. F. Dubremetz and K. Hager for sharing reagents. The Nikon Imaging Center at the University of Heidelberg we acknowledge for access to microscopes and technical assistance. We thank S. Münter for technical support of live imaging microscopy and all members of the lab for helpful discussions. DJPF is supported by an equipment grant from the Wellcome Trust. P.J.B. is supported by a NIH Grant (1R01AI064616). MM and MSB are supported by the “BioFuture-Programm” (Grant number: 0311897) of the Federal Ministry of Education and Research (BMBF).

References

1. Carruthers V, Boothroyd JC. Pulling together: an integrated model of Toxoplasma cell invasion. Curr Opin Microbiol. 2007; 10:83–89. [PubMed: 16837236]
2. Sheiner L, Soldati-Favre D. Protein trafficking inside Toxoplasma gondii. Traffic. 2008; 9:636–646. [PubMed: 18331382]
3. Ngo HM, Yang M, Paprotka K, Pypaert M, Hoppe H, Joiner KA. AP-1 in Toxoplasma gondii mediates biogenesis of the rhoptry secretory organelle from a post-Golgi compartment. J Biol Chem. 2003; 278:5343–5352. [PubMed: 12446678]
4. Harper JM, Huynh MH, Coppens I, Parussini F, Moreno S, Carruthers VB. A cleavable propeptide influences Toxoplasma infection by facilitating the trafficking and secretion of the TgMIC2-M2AP invasion complex. Mol Biol Cell. 2006; 17:4551–4563. [PubMed: 16914527]
5. El Hajj H, Papoin J, Cerede O, Garcia-Reguet N, Soete M, Dubremetz JF, Lebrun M. Molecular signals in the trafficking of Toxoplasma gondii protein MIC3 to the micronemes. Eukaryot Cell. 2008; 7:1019–1028. [PubMed: 18390648]
6. Dacks JB, Marinets A, Doolittle WF, Cavalier-Smith T, Logsdon JM Jr. Analyses of RNA Polymerase II genes from free-living protists: Phylogeny, Long Branch Attraction, and the Eukaryotic Big Bang. Molecular Biology and Evolution. 2002; 19:830–840. [PubMed: 12032239]
7. Langsley G, van Noort V, Carret C, Meissner M, de Villiers EP, Bishop R, Pain A. Comparative genomics of the Rab protein family in Apicomplexan parasites. Microbes Infect. 2008; 10:462–470. [PubMed: 18468471]
8. Kats LM, Cooke BM, Coppel RL, Black CG. Protein trafficking to apical organelles of malaria parasites - building an invasion machine. Traffic. 2008; 9:176–186. [PubMed: 18047549]
9. Nishi M, Hu K, Murray JM, Roos DS. Organellar dynamics during the cell cycle of Toxoplasma gondii. J Cell Sci. 2008; 121:1559–1568. [PubMed: 18411248]
10. Dubremetz JF. Rhoptries are major players in Toxoplasma gondii invasion and host cell interaction. Cell Microbiol. 2007; 9:841–848. [PubMed: 17346309]
11. Striepen B, Jordan CN, Reiff S, van Dooren GG. Building the perfect parasite: cell division in apicomplexa. PLoS Pathog. 2007; 3:e78. [PubMed: 17604449]
12. Karsten V, Qi H, Beckers CJ, Reddy A, Dubremetz JF, Webster P, Joiner KA. The protozoan parasite Toxoplasma gondii targets proteins to dense granules and the vacuolar space using both conserved and unusual mechanisms. J Cell Biol. 1998; 141:1323–1333. [PubMed: 9628889]
13. Praefcke GJ, McMahon HT. The dynamin superfamily: universal membrane tubulation and fission molecules? Nat Rev Mol Cell Biol. 2004; 5:133–147. [PubMed: 15040446]
14. Hinshaw JE. Dynamin and its role in membrane fission. Annu Rev Cell Dev Biol. 2000; 16:483–519. [PubMed: 11031245]
15. Danino D, Hinshaw JE. Dynamin family of mechanoenzymes. Curr Opin Cell Biol. 2001; 13:454–460. [PubMed: 11454452]
16. Elde NC, Morgan G, Winey M, Sperling L, Turkewitz AP. Elucidation of clathrin-mediated endocytosis in tetrahymena reveals an evolutionarily convergent recruitment of dynamin. PLoS Genet. 2005; 1:e52. [PubMed: 16276403]
17. Becker B, Melkonian M. The secretory pathway of protists: spatial and functional organization and evolution. Microbiol Rev. 1996; 60:697–721. [PubMed: 8987360]
18. Porchet-Hennere E, Nicolas G. Are rhoptries of Coccidia really extrusomes? J Ultrastruct Res. 1983; 84:194–203. [PubMed: 6632053]

19. Gao H, Kadirjan-Kalbach D, Froehlich JE, Osteryoung KW. ARC5, a cytosolic dynamin-like protein from plants, is part of the chloroplast division machinery. Proc Natl Acad Sci U S A. 2003; 100:4328–4333. [PubMed: 12642673]
20. Pfluger SL, Goodson HV, Moran JM, Ruggiero CJ, Ye X, Emmons KM, Hager KM. Receptor for retrograde transport in the apicomplexan parasite Toxoplasma gondii. Eukaryot Cell. 2005; 4:432–442. [PubMed: 15701805]
21. Herskovits JS, Burgess CC, Obar RA, Vallee RB. Effects of mutant rat dynamin on endocytosis. J Cell Biol. 1993; 122:565–578. [PubMed: 8335685]
22. Herm-Gotz A, Agop-Nersesian C, Munter S, Grimley JS, Wandless TJ, Frischknecht F, Meissner M. Rapid control of protein level in the apicomplexan Toxoplasma gondii. Nat Methods. 2007; 4:1003–1005. [PubMed: 17994029]
23. Black M, Arrizabalaga G, Boothroyd JC. Ionophore-Resistant Mutants of *Toxoplasma gondii* Reveal Host Cell Permeabilization as an Early Event in Egress. Mol Cell Biol. 2000; 20:9399–9408. [PubMed: 11094090]
24. Meissner M, Schluter D, Soldati D. Role of Toxoplasma gondii myosin A in powering parasite gliding and host cell invasion. Science. 2002; 298:837–840. [PubMed: 12399593]
25. Hakansson S, Morisaki H, Heuser J, Sibley LD. Time-lapse video microscopy of gliding motility in Toxoplasma gondii reveals a novel, biphasic mechanism of cell locomotion. Mol Biol Cell. 1999; 10:3539–3547. [PubMed: 10564254]
26. Hoppe HC, Ngo HM, Yang M, Joiner KA. Targeting to rhoptry organelles of Toxoplasma gondii involves evolutionarily conserved mechanisms. Nat Cell Biol. 2000; 2:449–456. taf/DynaPage.taf?file=/ncb/journal/v442/n447/full/ncb0700_0449.htmltaf/DynaPage.taf?file=/ncb/journal/v0702/n0707/abs/ncb0700_0449.html. [PubMed: 10878811]
27. Di Cristina M, Spaccapelo R, Soldati D, Bistoni B, Crisanti A. Two conserved amino acid motifs mediate protein targeting to the micronemes of the apicomplexan parasite *Toxoplasma gondii*. Mol Cell Biol. 2000
28. Brydges SD, Harper JM, Parussini F, Coppens I, Carruthers VB. A transient forward-targeting element for microneme-regulated secretion in Toxoplasma gondii. Biol Cell. 2008; 100:253–264. [PubMed: 17995454]
29. Soldati D, Lassen A, Dubremetz JF, Boothroyd JC. Processing of Toxoplasma ROP1 protein in nascent rhoptries. Mol Biochem Parasitol. 1998; 96:37–48. [PubMed: 9851605]
30. Bradley PJ, Boothroyd JC. The pro region of Toxoplasma ROP1 is a rhoptry-targeting signal. Int J Parasitol. 2001; 31:1177–1186. [PubMed: 11513886]
31. Taguchi N, Ishihara N, Jofuku A, Oka T, Mihara K. Mitotic phosphorylation of dynamin-related GTPase Drp1 participates in mitochondrial fission. J Biol Chem. 2007; 282:11521–11529. [PubMed: 17301055]
32. Huang JD, Cope MJ, Mermall V, Strobel MC, Kendrick-Jones J, Russell LB, Mooseker MS, Copeland NG, Jenkins NA. Molecular genetic dissection of mouse unconventional myosin-VA: head region mutations. Genetics. 1998; 148:1951–1961. [PubMed: 9560408]
33. van Dooren GG, Tomova C, Agrawal S, Humbel BM, Striepen B. Toxoplasma gondii Tic20 is essential for apicoplast protein import. Proc Natl Acad Sci U S A. 2008; 105:13574–13579. [PubMed: 18757752]
34. Donald RGK, Roos DS. Stable molecular transformation of *Toxoplasma gondii*: a selectable markerDHFR-TS marker based on drug resistance mutations in malaria. Proc Natl Acad Sci USA. 1993; 90:11703–11707. [PubMed: 8265612]
35. Carlton JM, Angiuoli SV, Suh BB, Kooij TW, Pertea M, Silva JC, Ermolaeva MD, Allen JE, Selengut JD, Koo HL, Peterson JD, Pop M, Kosack DS, Shumway MF, Bidwell SL, Shallom SJ, van Aken SE, Riedmuller SB, Feldblyum TV, Cho JK, Quackenbush J, Sedegah M, Shoaibi A, Cummings LM, Florens L, Yates JR, Raine JD, Sinden RE, Harris MA, Cunningham DA, Preiser PR, Bergman LW, Vaidya AB, van Lin LH, Janse CJ, Waters AP, Smith HO, White OR, Salzberg SL, Venter JC, Fraser CM, Hoffman SL, Gardner MJ, Carucci DJ. Genome sequence and comparative analysis of the model rodent malaria parasite Plasmodium yoelii yoelii. Nature. 2002; 419:512–519. [PubMed: 12368865]

36. Kessler H, Herm-Gotz A, Hegge S, Rauch M, Soldati-Favre D, Frischknecht F, Meissner M. Microneme protein 8--a new essential invasion factor in Toxoplasma gondii. J Cell Sci. 2008; 121:947–956. [PubMed: 18319299]

37. Donald RG, Roos DS. Stable molecular transformation of Toxoplasma gondii: a selectable dihydrofolate reductase-thymidylate synthase marker based on drug-resistance mutations in malaria. Proc Natl Acad Sci U S A. 1993; 90:11703–11707. [PubMed: 8265612]

38. Hettmann C, Herm A, Geiter A, Frank B, Schwarz E, Soldati T, Soldati D. A Dibasic Motif in the Tail of a Class XIV Apicomplexan Myosin Is an Essential Determinant of Plasma Membrane Localization. Mol Biol Cell. 2000; 11:1385–1400. [PubMed: 10749937]

39. Bradley PJ, Ward C, Cheng SJ, Alexander DL, Coller S, Coombs GH, Dunn JD, Ferguson DJ, Sanderson SJ, Wastling JM, Boothroyd JC. Proteomic analysis of rhoptry organelles reveals many novel constituents for host-parasite interactions in Toxoplasma gondii. J Biol Chem. 2005; 280:34245–34258. [PubMed: 16002398]

40. Schmidt HA, Strimmer K, Vingron M, von Haeseler A. TREE-PUZZLE: maximum likelihood phylogenetic analysis using quartets and parallel computing. Bioinformatics. 2002; 18:502–504. [PubMed: 11934758]

41. Page RD. TreeView: an application to display phylogenetic trees on personal computers. Comput Appl Biosci. 1996; 12:357–358. [PubMed: 8902363]

42. Robibaro B, Stedman TT, Coppens I, Ngo HM, Pypaert M, Bivona T, Nam HW, Joiner KA. Toxoplasma gondii Rab5 enhances cholesterol acquisition from host cells. Cell Microbiol. 2002; 4:139–152. [PubMed: 11906451]

43. Morrissette NS, Murray JM, Roos DS. Subpellicular microtubules associate with an intramembranous particle lattice in the protozoan parasite Toxoplasma gondii. J Cell Sci. 1997; 110:35–42. [PubMed: 9010782]

44. Mann T, Beckers C. Characterization of the subpellicular network, a filamentous membrane skeletal component in the parasite *Toxoplasma gondii*. Mol Biochem Parasitol. 2001; 115:257–268. [PubMed: 11420112]

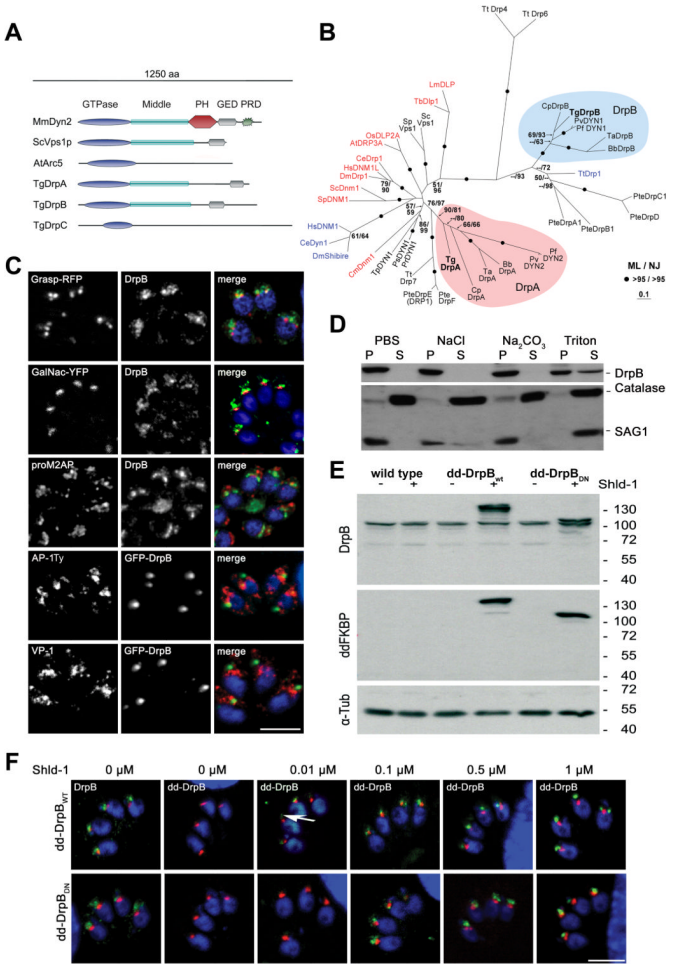

Figure 1. DrpB belongs to a ciliate specific class and localises close to the Golgi

(A) Scheme of different representative of the dynamin family, including *T. gondii* DrpA,B,C. Three representatives of dynamin proteins are shown considering their domain architecture (Sc: *Saccharomyces cerevisiae;* Mm: *Mus musculus;* At: *Arabidopsis thaliana)*. (**B)** Phylogenetic analysis of DrpA and DrpB reveals that they belong to unrelated classes. The figure shows an unrooted Maximum Likelihood phylogenetic tree (Ln Likelihood = −33260.47) in which bootstrap values >50% based on Maximum Likelihood and Distance Matrix/Neighbor-Joining phylogenies are indicated on the respective branches. Dynamins required for endocytosis are indicated in blue and required for mitochondria division in red. DrpA and DrpB fall into two distinct clades (indicated in purple and blue respectively). The accession numbers and the alignment can be downloaded as supporting information (Bb: *Babesia bovis;* Ce: *Caenorhabditis elegans;* Cm: *Cyanidioschyzon merolae;* Cp: *Cryptosporidium parvum;* Cr: *Chlamydomonas reinhardtii;* Dm: *Drosophila melanogaster;* Hs:*Homo sapiens;* Lm:*Leishmania major;* Os:*Oryza sativa;* Pf:*Plasmodium falciparum;* Pr: *Phytophthora ramorum;* Ps: *Phytophthora sojae;* Pte: *Paramecium tetraurelia;* Pv: *Plasmodium vivax;* Sp: *Schizosaccharomyces pombe;* Ta: *Theileria annulata;* Tb: *Trypanosoma brucei;* Tg:*Toxoplasma gondii;* Tp: *Thalassiosira pseudonana;* Tt: *Tetrahymena thermophila*) **(C)** Immunofluorescence analysis of RH_{WT} parasites grown on HFF-monolayers, using the indicated antibodies (proM2AP and VP-1) or transiently expressing the indicated markers (GRASP-RFP, GalNac-YFP and AP-1Ty, GFP-DrpB).. Scale bar: 10 µm **(D)** Cell fractionation on wild type parasites. Extracellular parasites were

harvested and lysed under different conditions (PBS, PBS with 1 M NaCl, PBS with 0.1 M Na_2CO_3 (pH 11.5) and PBS with 2% Triton X-100) followed by ultracentrifugation. Supernatant (SN) and pellet (P) fractions were analyzed by western blot analysis with indicated antibodies. **(E)** Immunoblot analysis of clonal parasites transfected with dd-$DrpB_{WT}$ or dd-$DrpB_{DN}$. Both parasite strains express the respective fusion protein only in presence of Shld-1. The immunoblot was probed with the indicated antibodies. TUB1 served as a loading control. **(F)** $DrpB_{wt}$ and $DrpB_{DN}$ accumulate close to the Golgi even at low overexpression. Parasites expressing GRASP-RFP and dd-$DrpB_{wt}$ or dd-$DrpB_{DN}$ were treated for 3 hours with the indicated amount of Shld-1 before localisation of GRASP and DrpB was compared. In case of dd-$DrpB_{wt}$ a signal for GFP can detected even at 0.01 μM Shld-1 close to the Golgi (arrow). Left: parasites not treated with Shld-1 were analysed using DrpB-antibodies. Scale bar: 10 μm. DrpB is always shown in green colour in merged images.

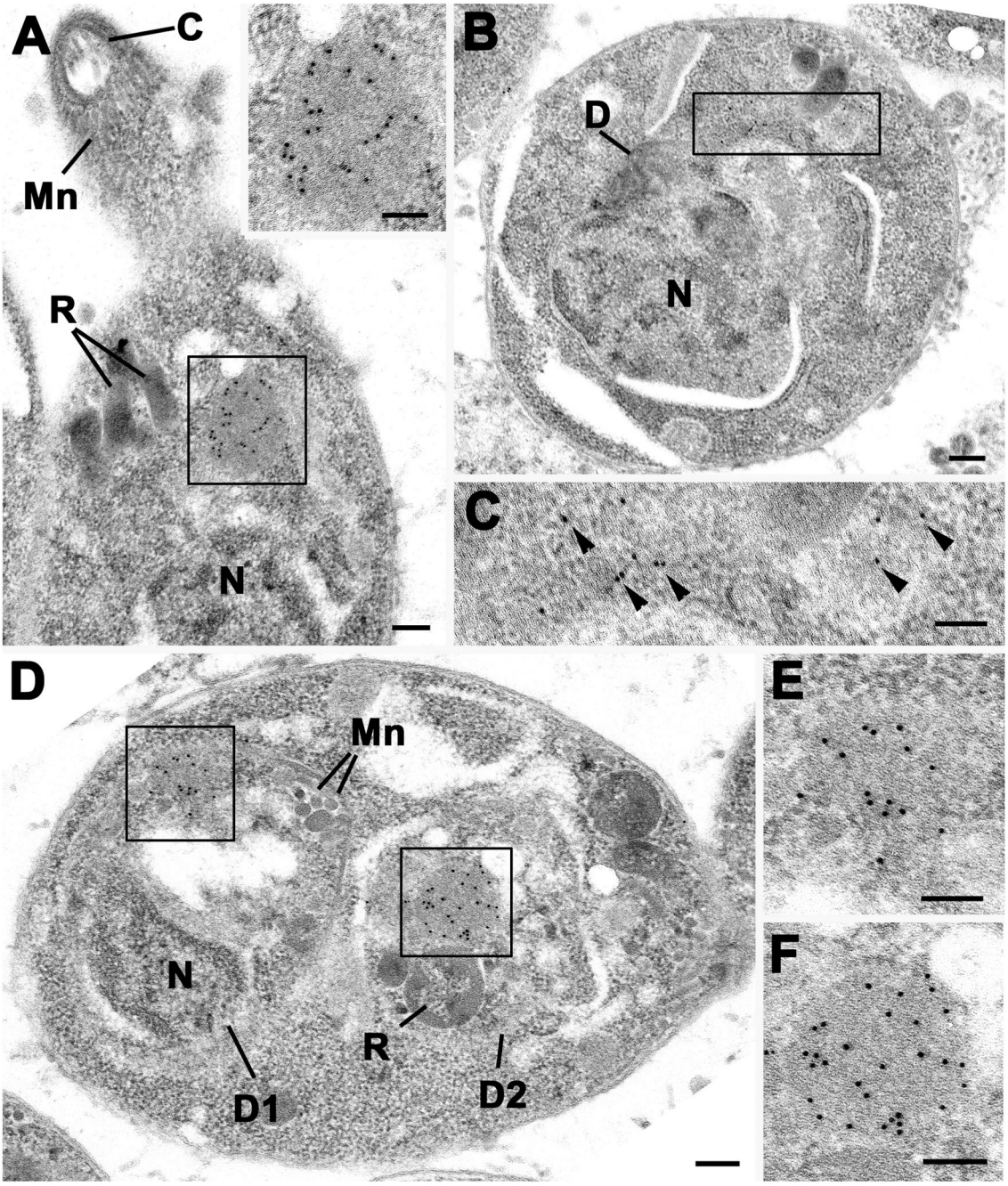

Figure 2. DrpB accumulates close to the Golgi

Electron micrographs of DrpB-GFP parasites immuno-stained with anti-GFP and visualised using 10 nm gold particles. **(A)** Longitudinal section through the anterior end of a tachyzoite showing a positively stained spherical structure (enclosed area) located between the nucleus (N) and rhoptries (R). Mn – microneme; C – conoid. **Insert.** Enlargement of the enclosed area in **a** showing the numerous gold particles located over the homogenous material. **(B)** Section through a tachyzoite at an early stage of proliferation showing early stage in formation of the daughter (D). N – nucleus. **(C)** Detail of the enclosed area in b showing the loss of the homogenous structure and dispersal of the gold particles (arrowheads). **(D)** Cross

section through a tachyzoite at a late stage of division showing the two daughters (D1, D2) containing rhoptries (R) and micronemes (Mn) within the mother cell cytoplasm. **(E, F)** Details of the two enclose areas in **D** showing the reformation of the homogenous structure labelled with gold particles within the daughter organisms. Bars represent 100 nm.

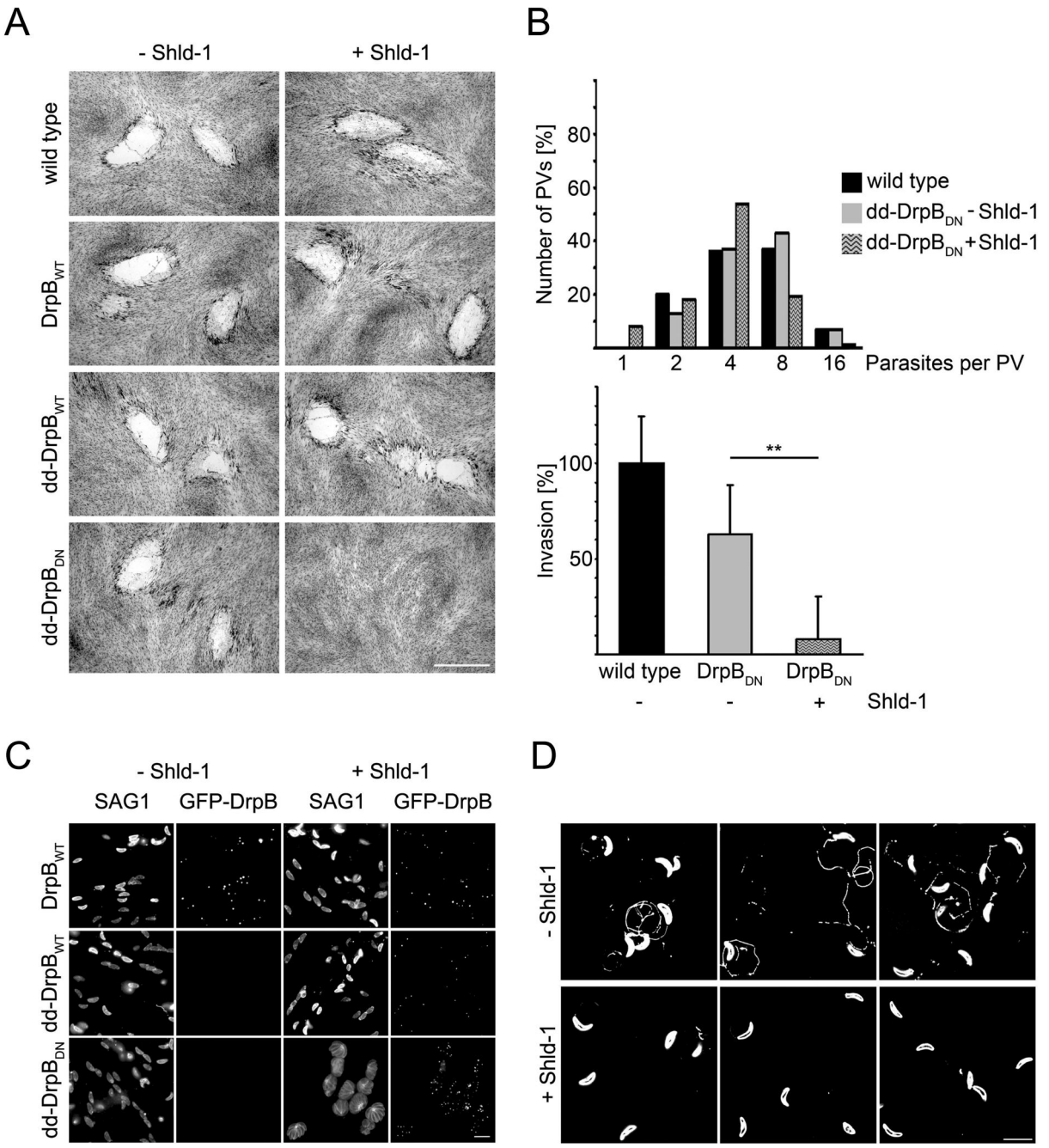

Figure 3. Phenotypic analysis of parasites expressing DrpB$_{DN}$

(A) Growth analysis of indicated parasite strains on HFF monolayers for 7 days. No plaque formation can be observed upon stabilisation of DrpB$_{DN}$. Scale bar: 1 mm **(B)** Replication (top) and invasion (bottom) assay of indicated parasite strains. Replication was analysed after 18 hours of continuous culture in the presence or absence of Shld-1. The depicted quantification is a representative of four independent experiments. For the invasion assay parasites were grown for 36 hours in presence or absence of Shld-1. Subsequently parasites were mechanically released from their host cell and equal numbers of parasites investigated considering their ability to invade new host cell. Invasion ability of RH$_{wt}$ parasites was

defined as 100% in each of the independent assays. Note that expression of dd-$DrpB_{wt}$ has no effect on invasion competency. Data represent mean values of three experiments ± s.d. Asterisks indicate significant difference ($P<0.01$ two-tailed Student's t-test) **(C)** Egress of the host cell is blocked upon expression of $DrpB_{DN}$. Indicated parasites were grown for 36 hours in presence or absence of Shld-1 and subsequently egress was triggered with A23187. After 15 minutes parasites were fixed and host cell lysis was analysed. Parasites expressing dd-$DrpB_{DN}$ are completely blocked in host cell egress. The depicted experiment has been repeated several times with the same result. Scale bar: 10 μm **(D)** Qualitative analysis of gliding motility. Parasites were treated as in b) and allowed to glide on a glass slide for 30 minutes before trail deposition was analysed with α-SAG1. Parasites expressing dd-$DrpB_{DN}$ are blocked in gliding. Occasionally short trails can be seen. The depicted image is a summary of three independent experiments. No difference in trail deposition was seen for RH or parasites expressing dd-$DrpB_{WT}$ (not shown). Scale bar: 10 μm.

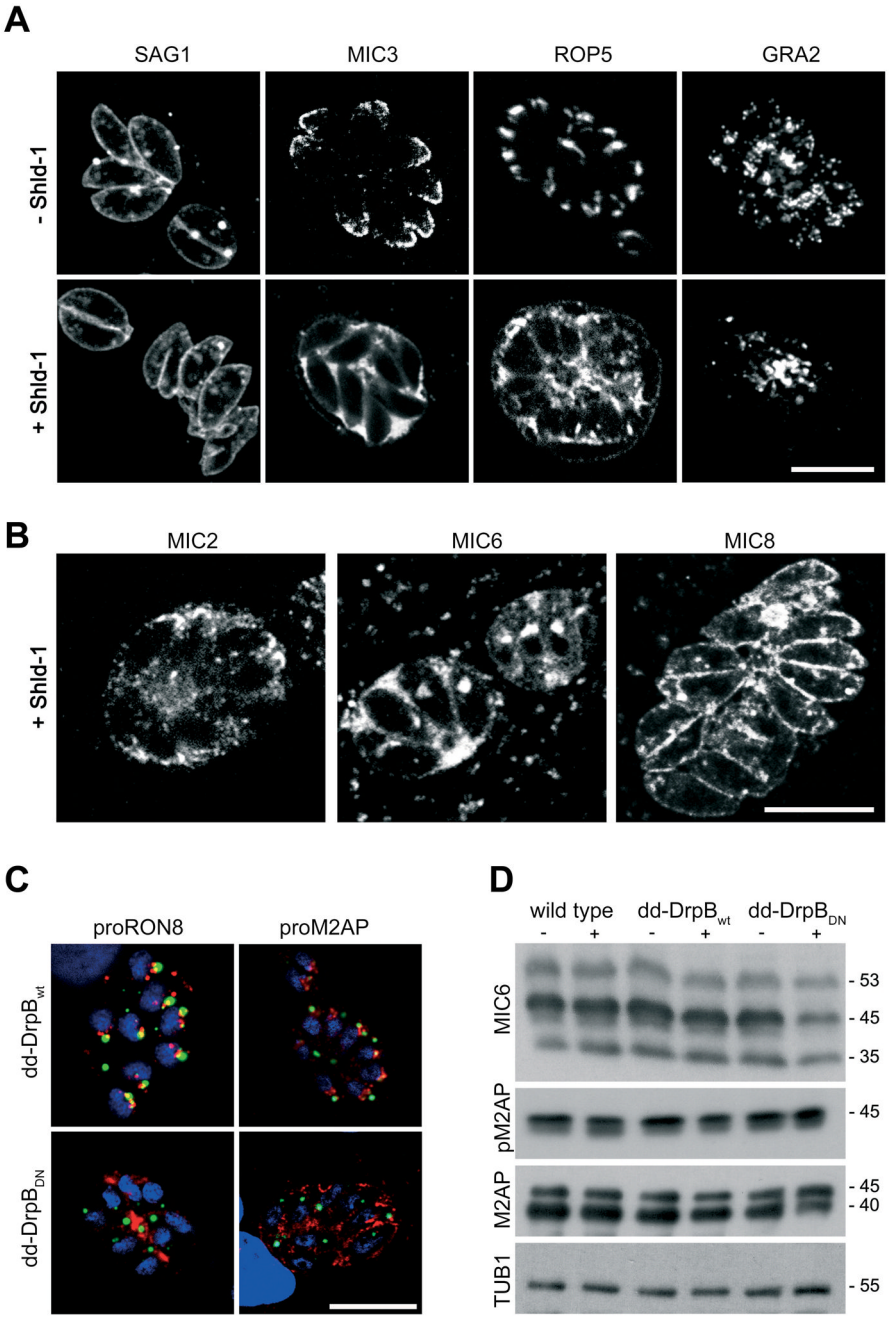

Figure 4. DrpB is required for the transport of secretory proteins

(A, B) Immunofluorescence analysis of dd-DrpB$_{DN}$-parasites grown in presence and absence of Shld-1 over night and stained with the indicated antibodies. **(C)** Immunofluorescence analysis of Shld-1 treated parasites expressing dd-DrpB$_{WT}$ and dd-DrpB$_{DN}$ for 24 hours in presence of Shld-1 and stained with indicated antibodies. Whereas expression of dd-DrpB$_{WT}$ does not interfere with the normal staining pattern of the endosomal associated compartments, in case of dd-DrpB$_{DN}$ expression the respective protein appears to be secreted into the lumen of the PV. Scale bar: 10 μm **(D)** Expression of dd-DrpB$_{DN}$ does not influence pro-peptide processing in intracellular parasites. For the immunoblot parasites were allowed to grow for 36 hours in presence or absence of Shld-1,

before lysate was prepared and probed with the indicated antibodies. Note that a weaker signal for the mature forms of MIC6 (45kDa) and M2AP (40 kDa) were detected in Shld-1 treated dd-DrpB$_{DN}$ parasites (−/+ Shld-1; molecular weights are indicated). DrpB is always shown in green colour in merged images.

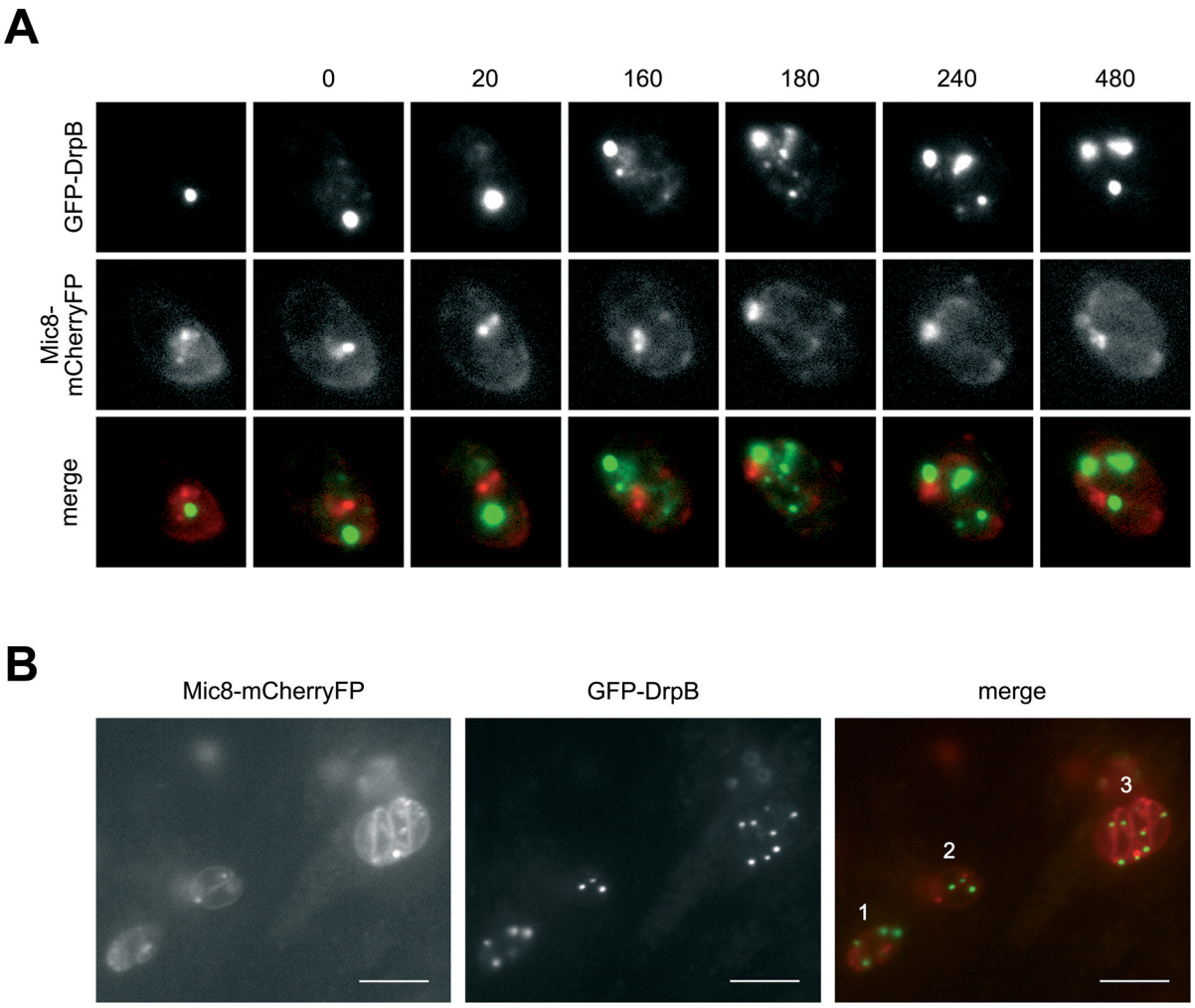

Figure 5. Time lapse analysis of parasites expressing DrpB$_{DN}$

(A) Parasites co-expressing dd-DrpB$_{DN}$ and MIC8-mCherryFP were allowed to grow for 8 hours on HFF cells in presence of Shld-1. After this time some PVs that contain two parasites already showed mislocalisation of MIC8-mCherryFP at the plasmamembrane (see also B). In contrast single parasites show normal localisation of MIC8-mCherry in the micronemes. Image acquisition was started when re-localisation of dd-DrpB$_{DN}$ became apparent (t=0). One image was taken every 20 minutes. During replication strong relocalisation of dd-DrpB$_{DN}$ was obvious and micronemal staining of the mother cell disappeared (t=0–160). Later MIC8-mCherry gets concentrated at the posterior pole of the nascent daughter cells close but distinct to the location of dd-DrpB$_{DN}$ (t=180). After completion of division dd-DrpB$_{DN}$ accumulates in discrete spots within the two daughter cells with a significant amount also detectable at the posterior pole of the parasite (see also Fig. 3c). No staining of micronemes is detectable after replication in the mature daughter parasites (t=240–480). See also supplementary movie. **(B)** Endpoint of an analogous experiment. In this image three parasites are depicted. (1) parasite in the process of replication with correct localisation of MIC8-mCherry in the mother cell still detectable (note the more diffuse staining of DrpB). (2) parasites already completed one replication cycle. MIC8-mCherry shows accumulation at the posterior pole and localisation at the surface of the mature daughter parasites. In (3) the parasites completed two rounds of

replication. MIC8-mCherry is found only at the surface of the parasites with no microneme staining detectable. Scale bar: 10 μm

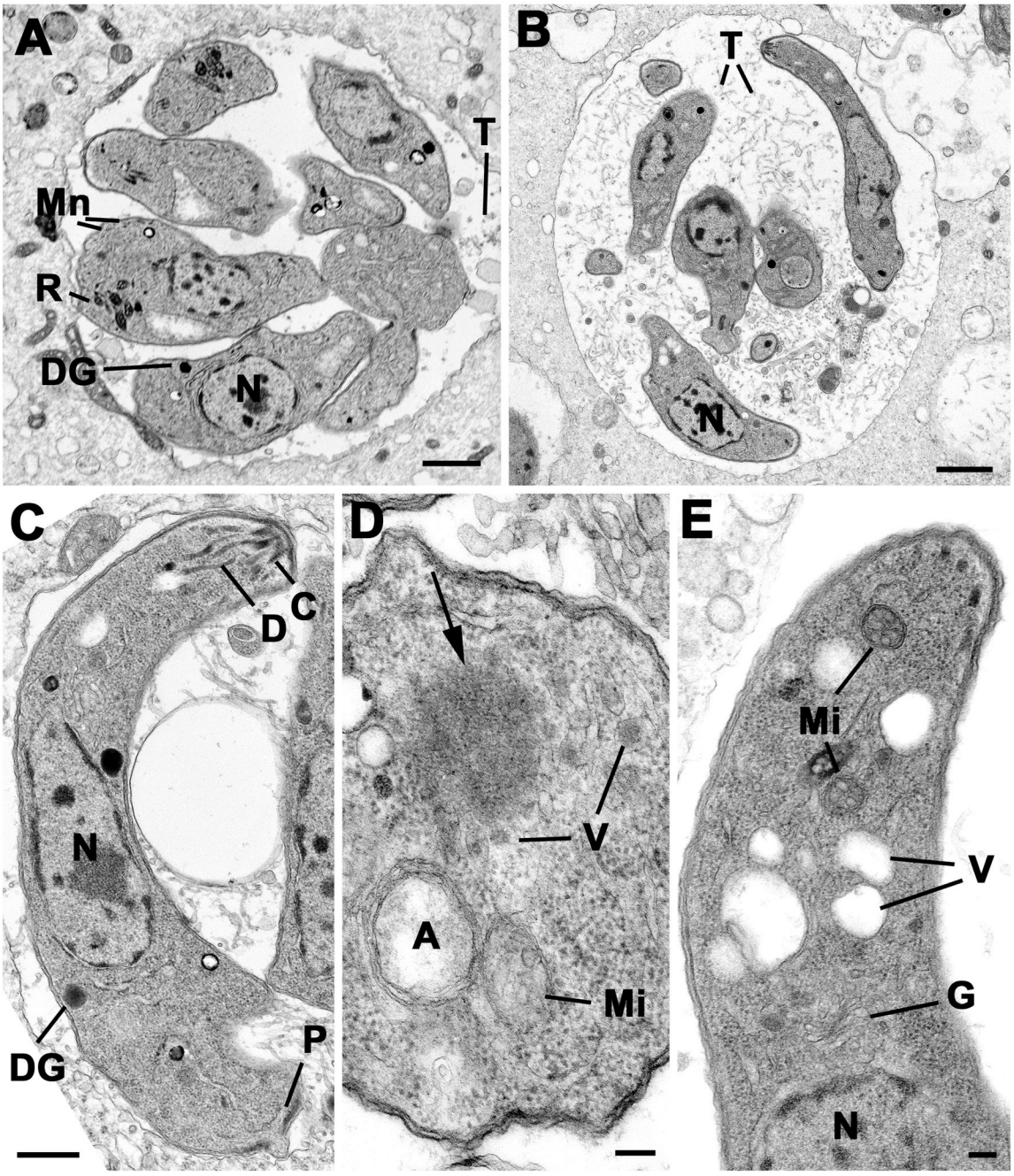

Figure 6. Transmission electron micrographs of control and treated intracellular parasites

(A) Low power of a group of tachyzoites from the untreated control sample at 36 hours showing the parasites located within a relatively tight PV with few intra-vacuolar tubules (T). The tachyzoites have a central nucleus (N) and apical organelles consisting of rhoptries (R), micronemes (Mn) and dense granules (DG). Scale Bar is 1 μm. **(B)** Low power from at treated sample (36 hours) showing the parasites located within a loose PV with numerous intra-vacuolar tubules (T). Note the elongated appearance of the tachyzoites and the lack of apical organelles. N- nucleus. Bar is 1 μm. **(C)** Longitudinal section through a Shld-1 treated tachyzoites showing the centrally located nucleus (N), the conoid (C) and associated duct-

like structures (D). Note the absence of rhotries and micronemes. DG – dense granule; P – posterior pore. Bar is 500 nm. **(D)** Cross-section through the anterior cytoplasm of a Shld-1 treated tachyzoite in which the apicoplast (A) and mitochondrion (Mi) can be seen. Note the homogenous electron dense structure (arrow) with surrounding vesicles (V). Bar is 100 nm. **(E)** Longitudinal section through the anterior of a Shld-1 treated tachyzoite illustrating a number of electron lucent vacuoles (V) located anterior to the Golgi body (G). N – nucleus; Mi – mitochondrion. Bar is 100 nm.